ARTICLES

Solvent Reorganization in Long-Range Electron Transfer: Density Matrix Approach

Akira Okada, Vladimir Chernyak, and Shaul Mukamel*

Department of Chemistry, University of Rochester, P.O. RC Box 270216, Rochester, New York 14627-0216

Received: September 5, 1997; In Final Form: December 5, 1997

The dynamics of charge transfer from a photoexcited donor to an acceptor coupled through a bridge is investigated by using a correlation-function approach in Liouville space that takes into account solvent dynamics with an arbitrary distribution of time scales. The time- and frequency-resolved fluorescence spectrum from the acceptor is used to probe the scaling of the ET rate with bridge size. The crossover between the coherent tunneling (transfer) and the incoherent sequential (transport) regimes and its implications on the nature of ET processes in DNA are discussed.

I. Introduction

Many important chemical and biological processes involve long-range transfer of energy or charge carriers (electrons and holes). Intense experimental and theoretical effort has been devoted to exploring how the transfer rate depends on the nature of the bridge connecting the donor and the acceptor.[1−6] Several recent experiments have focused on electron transfer (ET) in DNA,[7−13] which is involved in DNA damage and repair mechanisms.[14] Electron and energy transport through DNA is used in sequence-specific DNA probes currently being developed.[15] It has long been recognized that charge transfer in a donor/bridge/acceptor system may proceed in two distinct mechanisms. When the bridge energy is much higher than the donor and acceptor, its role is simply to mediate the coupling V_{DA} between them. The electron tunnels from the donor to the acceptor, and the bridge population is negligible at all times. This is known as the superexchange mechanism. A perturbative calculation of the electron tunneling matrix element V_{DA} was first made by McConnell.[16] In the opposite limit when the donnor/acceptor and bridge energies are closer than ∼kT, the bridge acts as a quantum wire and the electron hops through the bridge. This sequential electron transport mechanism has been studied extensively in, for example, doped polymers.[17] V_{DA} decreases exponentially with the distance R between the donor and the acceptor, $\sim\exp(-\beta R/2)$, and the resulting ET rate k_{ET} is proportional to $\exp(-\beta R)$. The value of the exponent β for ET in DNA is controversial, with experimental estimates varying between 0.2 $Å^{-1}$ [7,8] and 0.9 $Å^{-1}$.[9,10,13] ET rate of 1.6×10^6 s^{-1} has been reported for an eight-base-pair bridge with donor−acceptor separation of 21 Å.[13] A 2.5×10^6 s^{-1} rate was found in a different system (six base pairs, 17-Å separation).[9,10] These relatively slow rates suggest an exponent $\beta \sim 1.2-1.6$ $Å^{-1}$, similar to that found in proteins. Recent calculations of V_{DA} for ET in DNA using the semiemperical complete neglect of differential overlap (CNDO) method[18] and neglecting dynamical effects of nuclear degrees of freedom are consistent with these observations. In contrast, the unusually rapid ET rate 3.0×10^9 s^{-1} (40 Å, 15 base pairs) reported in ref 7 suggests a much smaller value of β (0.2 $Å^{-1}$). This has been attributed to sequential hopping (transport), where the DNA molecule may act as a quantum wire,[8,19] since the sequential mechanism results in a much weaker distance dependence of the rate.

Hu and Mukamel have shown that by formulating the problem of long-range electron transfer using the density matrix, it is possible to incorporate both mechanisms into a single unified theoretical framework.[20] The process may then be analyzed using Liouville space pathways. The superexchange (sequential) mechanism proceeds through off-diagonal (diagonal) density matrix elements in the site representation. The competition between the two mechanisms drew much attention in the context of the primary charge separation in the photosynthetic reaction center,[25,26] where a single chlorophyll molecule serves as a bridge between the special pair and the bacteriopheophytin.

Using the site representation for the electronic states and assuming that each molecule (donor, acceptor, and bridge) interacts independently with the solvent, it is possible to calculate the electron-transfer rate perturbatively in the intermolecular hopping integral. Coupling with the solvent can then be incorporated rigorously and nonperturbatively. The problem with this approach is that the number of necessary Liouville space pathways increases very rapidly with the bridge size. Higher order contributions in electronic couplings among sites are required to calculate the superexchange transfer from the donor to the acceptor in these theories. For example, for a system whose electronic structure can be modeled by an N-site one-dimensional tight binding Hamiltonian (the end sites are the donor and the acceptor), the superexchange ET rate is represented by the $2(N-1)$th order term in the electronic couplings between sites. For long bridges, higher order terms must be included, resulting in a large number of Liouville space pathways. Because of this difficulty, numerical calculations based on this expansion were limited to a three-site system. The competition between the two mechanisms was discussed for systems with more than three sites,[24] by neglecting nuclear degrees of freedom, using projection operator techniques. The density matrix approach has been recently applied to calculate the time evolution of ET in DNA including nuclear dynamics by applying the Redfield equations of motion.[19] The Redfield

S1089-5639(97)02918-6 CCC: $15.00
Published on Web 02/04/1998

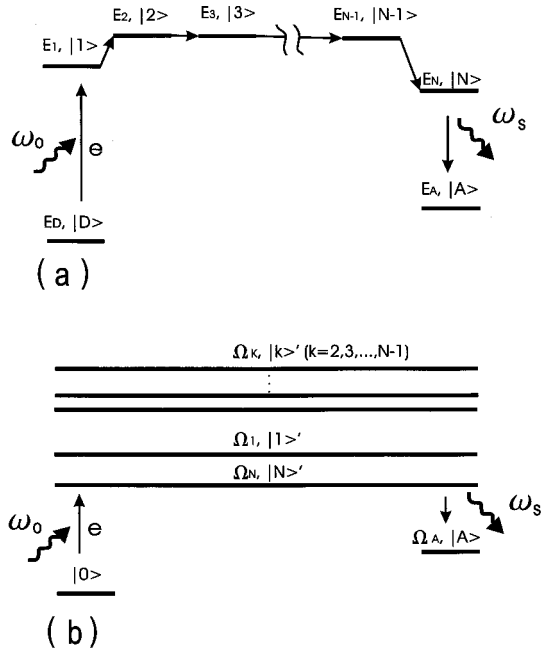

Figure 1. Electronic structure of the donor/bridge/acceptor system (a) in the site representation and (b) in the delocalized eigenstate representation. The delocalized states are denoted $|k\rangle \equiv B_k^\dagger|0\rangle$.

superoperator was calculated perturbatively in the coupling with the solvent. Consequently, this approach does not incorporate the solvent reorganization energies, which are required for a complete theoretical description of electron transport. In particular it does not reduce to the Marcus theory in the proper limit.

In this paper we extend the density matrix theory of photoinduced charge transfer in a donor/bridge/acceptor system,[20−24] to incorporate the reorganization energy, taking into account a realistic model for nuclear dynamics with an arbitrary distribution of time scales. The nuclear degrees of freedom are modeled as a continuous distribution of harmonic oscillators. All nuclear properties that affect the electronic degrees of freedom are contained in the spectral densities which describe the coupling of nuclear degrees of freedom to electronic populations in the site (real space) representation. By using the delocalized molecular orbital basis set, the number of Liouville space paths is greatly reduced. The present theory is nonperturbative in the electronic couplings among sites and in the coupling to solvent and applies even when the donor or the acceptor is strongly coupled to the bridge. It thus reproduces all the known limiting cases for the rate, including the Marcus theory.

We found that ET is governed by the superexchange mechanism for shorter bridges and by the sequential mechanism for longer bridges. The effects of the bridge size, the energy gap between the donor/acceptor and the bridge, the reorganization energies, and the temperature on the competition between these two mechanisms are investigated. Time-resolved and time- and frequency-resolved fluorescence from the acceptor following an optical excitation of the donor are calculated. Both excitation and emission processes are treated microscopically without invoking the standard assumption that the excited donor state is equilibrated initially. The signal has two contributions: a short-time coherent process, representing a direct excitation of the acceptor by the radiation field, and a long-time, incoherent process. Only the latter can be described by a simple rate equation. The short-time component may be neglected when nuclear relaxation is fast compared with the ET rate. This corresponds to an assumption that the nuclei are equilibrated with the initial distribution of electronic states. Although this assumption is used in the present numerical calculations, the formulation applies to slow nuclear relaxation as well.

The plan of this paper is as follows: The Hamiltonian for the donor/bridge/acceptor ET system is presented in section II. In section III we calculate the time- and frequency-resolved fluorescence signal from the acceptor following excitation of the donor. Simplified expressions for measurements conducted with a short (impulsive) pulse are derived in section IV. The spectral-diffusion limit is considered in section V. The numerical studies presented in section VI demonstrate the competition between the tunneling and the sequential mechanisms. These calculations use typical parameters employed in current experiments on DNA charge transfer. Finally our results are summarized in section VII.

II. Hamiltonian and Nuclear Spectral Densities

We consider a system consisting of a donor and an acceptor coupled though a bridge (Figure 1a). We denote the state where the transferring electron is on the nth molecule by $|n\rangle$ and its energy E_n'. $|1\rangle$ and $|N\rangle$ represent an electronically excited state of the donor and acceptor, respectively and $|n\rangle$ ($n = 2, 3, ..., N - 1$) are bridge states. The donor and the acceptor ground states will be denoted by $|D\rangle$ and $|A\rangle$, respectively. The hopping integral between the mth and nth molecules is V_{mn}. We assume that each molecule is coupled to its own harmonic bath, and the molecular Hamiltonian is

$$H \equiv \sum_{n=1}^{N} E_n|n\rangle\langle n| + \sum_{mn}^{m\neq n} V_{mn}|m\rangle\langle n| + \sum_{n=1}^{N}\sum_{j}\left(\frac{{p_{jn}}^2}{2m_{jn}} + \frac{m_{jn}{\omega_{jn}}^2{q_{jn}}^2}{2} - m_{jn}{\omega_{jn}}^2 d_{jn} q_{jn}|n\rangle\langle n|\right) + E_D|D\rangle\langle D| - \sum_j m_{j1}{\omega_{j1}}^2 d_{jD} q_{j1}|D\rangle\langle D| + E_A|a\rangle\langle A| - \sum_j m_{jN}{\omega_{jN}}^2 d_{jA} q_{jN}|A\rangle\langle A| \quad (2.1)$$

where p_{jn}, q_{jn}, m_{jn}, and d_{jn} are the momentum operator, the coordinate, the mass, the frequency, and the displacement of the jth oscillator coupled to the nth molecule.

The total Hamiltonian representing the system interacting with the radiation field $\epsilon(t)$ is

$$H_T(t) \equiv H - \epsilon(t)P \quad (2.2)$$

We assume that only the donor and the acceptor are coupled to the radiation field, and the polarization (dipole) operator is given by

$$P \equiv P_D + P_A \quad (2.3)$$

$$P_D \equiv \mu_D(|D\rangle\langle 1| + |1\rangle\langle D|) \quad (2.4)$$

$$P_A \equiv \mu_A(|A\rangle\langle N| + |N\rangle\langle A|) \quad (2.5)$$

Initially the system is in its ground state $|D\rangle$, which is therefore denoted $|0\rangle$. To decouple the bath in the initial (ground) state, we apply a transformation $q_{j1}' \equiv q_{j1} - d_{jD}$ and recast the Hamiltonian in the form

$$H = \sum_n \Omega'_n B_n^\dagger B_n + \sum_{mn}^{m\neq n} V_{mn} B_m^\dagger B_n + \Omega_A Y^\dagger Y - \sum_n (q_n^{(c)} - q_D^{(c)}) B_n^\dagger B_n - (q_A^{(c)} - q_D^{(c)}) Y^\dagger Y + H_{ph} \quad (2.6)$$

where we introduced operators $B_n \equiv |D\rangle\langle n|$, $Y \equiv |D\rangle\langle A|$, $\Omega'_n \equiv E_n - E_D + \sum_j m_{j1}\omega_{j1}^2(d_{jD}^2 - \delta_{n1}d_{j1}d_{jD})$, *and* $\Omega_A \equiv E_A - E_D + \sum_j m_{j1}\omega_{j1}^2 d_{jD}^2$. H_{ph} is the bath Hamiltonian,

$$H_{ph} \equiv \sum_{n=1}^{N}\sum_j \left(\frac{p_{jn}^2}{2m_{jn}} + \frac{m_{jn}\omega_{jn}^2 q_{jn}^2}{2}\right) \quad (2.7)$$

and the collective coordinates $q^{(c)}$ are defined by

$$q_n^{(c)} \equiv \sum_j m_{jn}\omega_{jn}^2 d_{jn} q_{jn}$$
$$q_D^{(c)} \equiv \sum_j m_{j1}\omega_{j1}^2 d_{jD} q_{j1}$$
$$q_A^{(c)} \equiv \sum_j m_{jN}\omega_{jN}^2 d_{jA} q_{jN} \quad (2.8)$$

In eq 2.6 we have set the ground-state energy of the system $E_D - \sum_j (m_{j1}\omega_{j1}^2 d_{jD}^2/2)$ to zero. The collective coordinates defined by eq 2.8 are described by the spectral densities $C_n(\omega)$, $n = 1, ..., N$, $C_D(\omega)$, $C_A(\omega)$, $C_{1D}(\omega)$, and $C_{NA}(\omega)$,

$$C_n(\omega) \equiv \sum_j \frac{m_{jn}\omega_{jn}^3}{4} d_{jn}^2 2\pi[\delta(\omega - \omega_{jn}) - \delta(\omega + \omega_{jn})] \quad \text{for} \quad n = 1, 2, ..., N \quad (2.9)$$

$$C_D(\omega) \equiv \sum_j \frac{m_{j1}\omega_{j1}^3}{4} d_{jD}^2 2\pi[\delta(\omega - \omega_{j1}) - \delta(\omega + \omega_{j1})] \quad (2.10)$$

$$C_A(\omega) \equiv \sum_j \frac{m_{jN}\omega_{jN}^3}{4} d_{jA}^2 2\pi[\delta(\omega - \omega_{jN}) - \delta(\omega + \omega_{jN})] \quad (2.11)$$

$$C_{1D}(\omega) \equiv \sum_j \frac{m_{j1}\omega_{j1}^3}{4} d_{j1} d_{jD} 2\pi[\delta(\omega - \omega_{j1}) - \delta(\omega + \omega_{j1})] \quad (2.12)$$

$$C_{NA}(\omega) \equiv \sum_j \frac{m_{jN}\omega_{jN}^3}{4} d_{jN} d_{jA} 2\pi[\delta(\omega - \omega_{jN}) - \delta(\omega + \omega_{jN})] \quad (2.13)$$

Using this notation, the donor and acceptor dipole operators assume the form

$$P_D \equiv \mu_D(B_1^\dagger + B_1) \quad (2.14)$$

$$P_A \equiv \mu_A(Y^\dagger B_N + B_N^\dagger Y) \quad (2.15)$$

We next switch to the delocalized molecular orbital representation (see Figure 1b). To that end we consider the electronic Hamiltonian $\mathbf{H}^{(el)}$ consisting of first two terms in eq 2.27, $[\mathbf{H}^{(el)}]_{mn} \equiv \delta_{mn}\Omega'_m + (1 - \delta_{mn})V_{mn}$. We denote its normalized eigenfunctions $\psi_k(n)$ with energies Ω_k and introduce the exciton creation operators $B_k^\dagger$,

$$B_k^\dagger \equiv \sum_n \psi_k(n) B_n^\dagger \quad (2.16)$$

The Hamiltonian is recast in a form

$$H \equiv H_0 + H_1 \quad (2.17)$$

with

$$H_0 \equiv \sum_k \Omega_k B_k^\dagger B_k + \Omega_A Y^\dagger Y - \sum_k q_k^{(c)} B_k^\dagger B_k - q_Y^{(c)} Y^\dagger Y + H_{ph} \quad (2.18)$$

$$H_1 \equiv -\sum_{kk'}^{k\neq k'} q_{kk'}^{(c)} B_k^\dagger B_k \quad (2.19)$$

In eqs 2.18−2.26 k, k' label exciton states. The collective coordinates $q_Y^{(c)}$, $q_k^{(c)}$, and $q_{kk'}^{(c)}$ in the exciton representation are defined by

$$q_Y^{(c)} \equiv q_A^{(c)} - q_D^{(c)} \quad (2.20)$$

$$q_{kk'}^{(c)} \equiv \sum_n \psi_k(n)\,\psi_{k'}(n)(q_n^{(c)} - q_D^{(c)}) \quad (2.21)$$

and $q_k^{(c)} \equiv q_{kk}^{(c)}$. The corresponding spectral densities are given by

$$C_{kk',qq'}(\omega) = \sum_{mn} \psi_k(m)\,\psi_{k'}(m)\,\psi_q(n)\,\psi_{q'}(n)[\delta_{mn}C_m(\omega) + C_D(\omega) - \delta_{1n}C_{1D}(\omega) - \delta_{1m}C_{1D}(\omega)] \quad (2.22)$$

$$C_{kk',Y}(\omega) = \sum_n \psi_k(n)\,\psi_{k'}(n)[C_D(\omega) - \delta_{1n}C_{1D}(\omega) + \delta_{nN}C_{NA}(\omega)] \quad (2.23)$$

$$C_{YY}(\omega) = C_D(\omega) + C_A(\omega) \quad (2.24)$$

The dipole operators adopt the form

$$P_D \equiv \sum_k \mu_{Dk}(B_k^\dagger + B_k) \quad (2.25)$$

$$P_A \equiv \sum_k \mu_{Ak}(Y^\dagger B_k + B_k^\dagger Y) \quad (2.26)$$

with the dipole matrix elements

$$\mu_{Dk} \equiv \sum_k \mu_D \psi_k(1) \quad (2.27)$$

$$\mu_{Ak} \equiv \sum_k \mu_A \psi_k(N) \quad (2.28)$$

This Hamiltonian will be used in the coming sections.

III. Time- and Frequency-Resolved Fluorescence Signal

The Hamiltonian (eqs 2.17−2.26) is formally identical to that derived in ref 30 for molecular aggregates, where $B^\dagger$ denoted one-exciton creation operators, whereas $Y^\dagger$'s were creation operators for two-exciton states. In our case the $Y^\dagger$ operator moves an electron from the ground state of the donor to the ground state of the acceptor. However, the two Hamiltonians are formally identical, and all the results of ref 30 can be applied to the present problem.

The time- and frequency-resolved signal $S(t, \omega_s)$ can be represented in a form

$$S(t, \omega_s) = \int_{-\infty}^{\infty} d\tau e^{i\omega_s \tau} \tilde{S}(t, \tau) \tag{3.1}$$

with

$$\tilde{S}(t, \tau) \equiv \langle \tilde{P}_A(t + \tau)\, \tilde{P}_A(t) \rangle \tag{3.2}$$

where for any operator B we define the Heisenberg operator $\tilde{B}(t)$ whose evolution is determined by the total Hamiltonian H_T. The simpler time-resolved signal $I(t)$ is given by

$$I(t) \equiv \int d\omega_s S(t, \omega_s) = \langle \tilde{P}_A(t)\, \tilde{P}_A(t) \rangle \tag{3.3}$$

Expanding the expectation value in the rhs of eq 3.1 to second order in the driving field $\epsilon(t)$ and invoking the rotating wave approximation, $\tilde{S}(t, \tau)$ is expressed in terms of four-point correlation functions of the dipole operators,

$$\tilde{S}(t, \tau) \equiv \int_{-\infty}^{t} d\tau' \int_{-\infty}^{t+\tau} d\tau'' \langle P_D(\tau'')\, P_A(t + \tau) \times P_A(t)\, P_D(\tau') \rangle \frac{\epsilon(\tau')}{\hbar} \frac{\epsilon(\tau'')}{\hbar} \tag{3.4}$$

In contrast to eq 3.2, the time evolution is now determined by the free molecular Hamiltonian H (without the radiation field),

$$P(t) \equiv \exp\left(\frac{i}{\hbar} Ht\right) P \exp\left(-\frac{i}{\hbar} Ht\right) \tag{3.5}$$

Making use of eqs 2.25 and 2.26, we obtain

$$\tilde{S}(t, \tau) \equiv \int_{-\infty}^{t} d\tau' \int_{-\infty}^{t+\tau} d\tau''\, F_2(\tau'', t + \tau, t, \tau') \frac{\epsilon(\tau')}{\hbar} \frac{\epsilon(\tau'')}{\hbar} \tag{3.6}$$

where

$$F_2(\tau_4, \tau_3, \tau_2, \tau_1) \equiv \sum_{kk'qq'} \mu_{Dk} \mu_{Ak'} \mu_{Aq} \mu_{Dq'} \langle B_k(\tau_4)\, B_{k'}^{\dagger}(\tau_3)\, Y(\tau_3)\, Y^{\dagger}(\tau_2)\, B_q(\tau_2)\, B_{q'}^{\dagger}(\tau_1) \rangle \tag{3.7}$$

The correlation function in the rhs of eq 3.7 has been calculated in ref 30 using a perturbative expansion in H_1. Substituting the result of ref 30 into eq 3.7, we obtain

$$\tilde{S}(t, \tau) \equiv \theta(\tau) \sum_{kk'} \int_{-\infty}^{t} d\tau' \int_{-\infty}^{t'} d\tau''\, W_k^{L}(\tau)\, G_{kk'}(t - \tau') \times D_{k'}(\tau' - \tau'') \frac{\epsilon(\tau')}{\hbar} \frac{\epsilon(\tau'')}{\hbar} + \theta(-\tau) \sum_{kk'} \int_{-\infty}^{t+\tau} d\tau' \int_{-\infty}^{t'} d\tau'' \times W_k^{L}(\tau)\, G_{kk'}(t + \tau - \tau')\, D_{k'}(\tau' - \tau'') \frac{\epsilon(\tau')}{\hbar} \frac{\epsilon(\tau'')}{\hbar} + \tilde{S}^{(st)}(t, \tau) \tag{3.8}$$

where

$$D_{k'}(t) \equiv D_{k'}^{L}(t) + D_{k'}^{L}(-t) \tag{3.9}$$

D^L is the doorway function representing the density matrix created upon optical excitation. W^L is a window function representing the detection process. $G_{kk'}$ is the Green function representing polaron population relaxation, and $\tilde{S}^{(st)}$ is the short-time component of the signal. These quantities can be expressed in terms of line-shape functions $g_{\mu\nu}(\tau)$ $\mu, \nu = kk'$, Y related to spectral densities $C_{\mu\nu}(\omega)$.

$$g_{\mu\nu}(\tau) \equiv \int_{-\infty}^{\infty} \frac{d\omega}{2\pi} \frac{C_{\mu\nu}(\omega)}{\hbar\omega^2} \left[(1 - \cos(\omega\tau)) \coth\left(\frac{\hbar\omega}{2k_B T}\right) + i(\sin(\omega\tau) - \omega\tau) \right] \tag{3.10}$$

All quantities are given in Appendix A.

The Green function $G_{kk'}(\tau)$ can be calculated by solving the master equation

$$\frac{d}{d\tau} G_{kk'}(\tau) = \sum_q K_{kq} G_{qk'}(\tau) \tag{3.11}$$

with $G_{kk'}(0) = \delta_{kk'}$, and the kernel

$$K_{qq'} \equiv \int_{-\infty}^{\infty} d\tau K_{qq'}^{L}(\tau) \quad \text{for} \quad q \neq q' \tag{3.12}$$

$$K_{qq} \equiv \sum_{q'}^{q'' \neq q} K_{q''q} \tag{3.13}$$

$K_{qq'}^{L}(\tau)$ has the form

$$K_{qq'}^{L}(\tau) = K_{qq'}^{(F)}(\tau) \left\{ \ddot{g}_{qq',q'q}(\tau) - \left[\dot{g}_{q'q,q'q'}(\tau) - \dot{g}_{q'q,qq}(\tau) + 2\frac{i}{\hbar} \lambda_{q'q,q'q'} \right] \times \left[\dot{g}_{q'q,qq'}(\tau) - \dot{g}_{qq,qq'}(\tau) + 2\frac{i}{\hbar} \lambda_{qq',q'q'} \right] \right\} \tag{3.14}$$

with

$$K_{qq'}^{(F)}(\tau) = \exp\left[-\frac{i}{\hbar} (\Omega_q - \Omega_{q'}) \tau - \bar{f}_{qq'}(\tau) \right] \tag{3.15}$$

and

$$\bar{f}_{qq'}(\tau) \equiv g_{qq,qq}(\tau) + g_{q'q',q'q'}(\tau) - g_{q'q',qq}(\tau) - g_{qq,q'q'}(\tau) + 2\frac{i}{\hbar} (\lambda_{q'q',q'q'} - \lambda_{qq,q'q'}) \tau \tag{3.16}$$

Equations 3.1 and 3.8−3.16 provide a closed expression for the time- and frequency-resolved fluorescence signal.

In concluding this section we present the expression for the simpler, time-resolved, signal (integrated over frequency) defined by eq 3.3. Using eqs 3.3, 3.8, and A3, it can be represented in the doorway/window form:

$$I(t) = \sum_{kk'} |\mu_{Ak}|^2 \int_{-\infty}^{t} d\tau' \int_{-\infty}^{\tau'} d\tau''\, G_{kk'}(t - \tau') \times D_{k'}(\tau' - \tau'') \frac{\epsilon(\tau')}{\hbar} \frac{\epsilon(\tau'')}{\hbar} + I^{(st)}(t) \tag{3.17}$$

with the short-time component

$$I^{(st)}(t) = \int_{-\infty}^{t} d\tau' \int_{-\infty}^{t} d\tau''\, F_2(\tau'', t, t, \tau') \frac{\epsilon(\tau')}{\hbar} \frac{\epsilon(\tau'')}{\hbar} - \sum_{k} |\mu_{Ak}|^2 \int_{-\infty}^{t} d\tau' \int_{-\infty}^{\tau'} d\tau''\, D_k(\tau' - \tau'') \frac{\epsilon(\tau')}{\hbar} \frac{\epsilon(\tau'')}{\hbar} \tag{3.18}$$

IV. Impulsive Signals Obtained with Short Excitation Pulses

The expressions for the signals derived in section III can be simplified considerably when the excitation pulse is short. We represent the driving electric field $\epsilon(\tau)$ in the form

$$\epsilon(\tau) = E(\tau) e^{-i\omega_0 \tau} + E^*(\tau) e^{i\omega_0 \tau} \tag{4.1}$$

where ω_0 is the carrier frequency of the exciting pulse and $E(\tau)$ is the envelope, which is slow compared to the carrier frequency ω_0: $t_0 \gg \omega_0^{-1}$, where t_0 is the pulse duration. We also assume that $t_0 \ll t_p$, where t_p is the time scale of population relaxation defined by the lowest nonzero mode of the master equation. The other two important time scales characterizing the system are the dephasing time t_d, determined by the time scale of $D(t)$ and $W(t)$, and the nuclear relaxation time scale t_n. We assume t_d, $t_n \ll t_p$, where the ratio of t_d and t_n may be arbitrary. The limits $t_d \ll t_n$ and $t_n \ll t_d$ are known as spectral diffusion and homogeneous limits respectively.[27]

We first consider the snapshot limit when $t_d \ll t_0 \ll t_p$. The signals are conveniently expressed in terms of the Fourier transforms of the doorway and window functions:

$$D_k(\omega) \equiv \int_{-\infty}^{\infty} d\tau e^{i\omega\tau} D_k^L(\tau) \tag{4.2}$$

$$W_k(\omega) \equiv \int_{-\infty}^{\infty} d\tau e^{i\omega\tau} W_k^L(\tau) \tag{4.3}$$

$D_k(\omega)$ and $W_k(\omega)$ represent the absorption and fluorescence spectra of the kth exciton, respectively. Substituting eq 4.1 into our expressions for the signals, we can then carry out the necessary integrations, which yields for the time- and frequency-resolved signal

$$S(t, \omega_s) = \sum_{kk'} W_k(\omega_s)\, G_{kk'}(t)\, D_{k'}(\omega_0) \int_{-\infty}^{\infty} d\tau' \frac{|E(\tau')|^2}{\hbar^2} + S^{(st)}(\omega_s, t) \tag{4.4}$$

The time-resolved signal is similarly given by

$$I(t) = \sum_{kk'} |\mu_{Ak}|^2 G_{kk'}(t)\, D_{k'}(\omega_0) \int_{-\infty}^{\infty} d\tau' \frac{|E(\tau')|^2}{\hbar^2} + I^{(st)}(t) \tag{4.5}$$

The expressions for the short-time components can be simplified further in the spectral diffusion limit $t_d \ll t_n$ and for snapshot excitation: $t_d \ll t_0 \ll t_p$[27] where they assume the form

$$I^{(st)}(t) = \left[\int_{-\infty}^{\infty} d\tau'\, F_2(0, t, t, \tau') e^{i\omega_0\tau'} - \sum_k |\mu_{Ak}|^2 D_{k'}(\omega_0)\right] \int_{-\infty}^{\infty} d\tau'' \frac{|E(\tau'')|^2}{\hbar^2} \tag{4.6}$$

$$S^{(st)}(\omega_s, t) = \left[\int_{-\infty}^{\infty} d\tau' \int_{-\infty}^{\infty} d\tau''\, F_2(0, t, t + \tau'', \tau') e^{i\omega_s\tau'' + i\omega_0\tau'} - \sum_k W_k(\omega_s)\, D_k(\omega_0)\right] \int_{-\infty}^{\infty} d\tau \frac{|E(\tau)|^2}{\hbar^2} \tag{4.7}$$

V. Spectral Diffusion Limit

In this section, using the overdamped Brownian oscillator model for the spectral density,[27] we derive closed expressions for the DW function, $D_{k'}(\omega)$, $W_k(\omega)$, and the kernel $K_{qq'}$. We assume that all collective bath coordinates have the same relaxation rate Λ,

$$C_n(\omega) = \frac{\lambda_n}{\lambda} C(\omega) \quad \text{for} \quad n = 1, 2, ..., N \tag{5.1}$$

$$C_D(\omega) = \frac{\lambda_D}{\lambda} C(\omega) \tag{5.2}$$

$$C_A(\omega) = \frac{\lambda_A}{\lambda} C(\omega) \tag{5.3}$$

where

$$\lambda_n \equiv \sum_j \frac{m_{jn}\omega_{jn}^2 d_{jn}^2}{2} \tag{5.4}$$

$$\lambda_D \equiv \sum_j \frac{m_{j1}\omega_{j1}^2 d_{jD}^2}{2} \tag{5.5}$$

$$\lambda_A \equiv \sum_j \frac{m_{jN}\omega_{jN}^2 d_{jA}^2}{2} \tag{5.6}$$

$$\lambda \equiv \frac{1}{N}\sum_{n=1}^{N} \lambda_n \tag{5.7}$$

$$C(\omega) \equiv 2\frac{\lambda\omega\Lambda}{\omega^2 + \Lambda^2} \tag{5.8}$$

with $d_{jD} = \sqrt{\lambda_D/\lambda_1}\, d_{j1}$ and $d_{jA} = \sqrt{\lambda_A/\lambda_N}\, d_{jN}$. For simplicity we assume that the reorganization energies are uncorrelated (i.e., each site has its own bath). This assumption may be relaxed without a major complication. All $g_{\mu,\nu}(t)$ are now expressed using a single function $g(t)$ as

$$g_{\mu,\nu}(t) = \frac{\lambda_{\mu,\nu}}{\lambda} g(t) \tag{5.9}$$

where

$$g(t) \equiv \int_{-\infty}^{\infty} \frac{d\omega}{2\pi} \frac{C(\omega)}{\omega^2} \left[(1 - \cos(\omega t)) \coth\left(\frac{\hbar\omega}{2k_B T}\right) + i(\sin(\omega t) - \omega t)\right] \tag{5.10}$$

and

$$\lambda_{kk',qq'} \equiv \sum_{mn} \psi_k(m)\, \psi_{k'}(m)\, \psi_q(n)\, \psi_{q'}(n)[\delta_{mn}\lambda_m + \lambda_D - (\delta_{1n} + \delta_{1m})\sqrt{\lambda_1\lambda_D}] \tag{5.11}$$

$$\lambda_{kk',Y} \equiv \sum_n \psi_k(n)\, \psi_{k'}(n)[\lambda_D - \delta_{1n}\sqrt{\lambda_1\lambda_D} + \delta_{nN}\sqrt{\lambda_N\lambda_A}] \tag{5.12}$$

$$\lambda_{YY} \equiv \lambda_D + \lambda_A \tag{5.13}$$

In the high-temperature limit, $k_B T \gg \hbar\Lambda$, using eqs 5.8 and 5.10 we have

$$g(t) \equiv z(e^{-\Lambda t} + \Lambda t - 1) \quad \text{for} \quad t \geq 0 \tag{5.14}$$

$$g(-t) = g^*(t) \tag{5.15}$$

where

$$z \equiv \left(\frac{2\lambda k_B T}{\hbar^2\Lambda^2} - i\frac{\lambda}{\hbar\Lambda}\right) \tag{5.16}$$

In the static limit, $2\lambda k_B T \gg (\hbar\Lambda)^2$, using eqs 3.12−3.16 and 5.11−5.16, we obtain

$$K_{qq'} = F_{qq'}\left(\frac{\pi\hbar^2}{\bar{\lambda}_{qq'}k_B T}\right)^{1/2} \exp\left[-\frac{(\bar{\Omega}_q - \bar{\Omega}_{q'} + \bar{\lambda}_{qq'})^2}{4\bar{\lambda}_{qq'}k_B T}\right] \quad (5.17)$$

where

$$F_{qq'} \equiv \frac{1}{\hbar^2}\left[\frac{(\bar{\Omega}_q - \bar{\Omega}_{q'})(\lambda_{q'q,q'q'} - \lambda_{q'q,qq}) - \bar{\lambda}_{qq'}(\lambda_{q'q,q'q'} + \lambda_{q'q,qq})}{\bar{\lambda}_{qq'}}\right]^2 + \frac{2k_B T}{\hbar^2}\left(\lambda_{qq',q'q} - \frac{(\lambda_{q'q,q'q'} - \lambda_{q'q,qq})^2}{\bar{\lambda}_{qq'}}\right) \quad (5.18)$$

with

$$\bar{\Omega}_q \equiv \Omega_q - \lambda_{qq,qq} \quad (5.19)$$

$$\bar{\lambda}_{qq'} \equiv \lambda_{qq,qq} + \lambda_{q'q',q'q'} - \lambda_{q'q',qq} - \lambda_{qq,q'q'} \quad (5.20)$$

Equations 5.17−5.18 satisfy the detailed balance condition, $K_{qq'}/K_{q'q} = \exp[-(\bar{\Omega}_q - \bar{\Omega}_{q'})/k_B T]$. In the same manner we obtain

$$D_k(\omega) = \mu_{Dk}^2\left(\frac{\pi\hbar^2}{\bar{\lambda}_k k_B T}\right)^{1/2} \exp\left[-\frac{(\Omega_k - \hbar\omega)^2}{4\bar{\lambda}_k k_B T}\right] \quad (5.21)$$

$$W_k(\omega) = \mu_{Ak}^2\left(\frac{\pi\hbar^2}{\bar{\lambda}_{Ak}k_B T}\right)^{1/2} \exp\left[-\frac{(\bar{\Omega}_A - \bar{\Omega}_k + \bar{\lambda}_{Ak} - \hbar\omega)^2}{4\bar{\lambda}_{Ak}k_B T}\right] \quad (5.22)$$

with

$$\bar{\lambda}_k \equiv \lambda_{kk,kk} \quad (5.23)$$

$$\bar{\lambda}_{Ak} \equiv \lambda_{kk,kk} + \lambda_{Y,Y} - 2\lambda_{kk,Y} \quad (5.24)$$

$$\bar{\Omega}_A = \Omega_A - \lambda_{Y,Y} \quad (5.25)$$

The complete expression for the rate matrix $K_{qq'}$ for the overdamped Brownian oscillator spectral density, which is not limited to the static limit, is given in Appendices B and C.

VI. Interplay or Tunneling and Sequential Transfer

The calculations presented in this section illustrate the range of parameters and time scales whereby the ET process can be considered either direct (tunneling) or hopping type. We have used typical parameters for DNA charge transfer and varied them over a broad range. These results show under what conditions a DNA bridge acts as a quantum wire. For the electronic parameters we used $E_D = -1.25$ eV, $E_A = -2.29$ eV, $E_1 = -0.25$ eV, $E_N = -0.29$ eV, $E_n = 0.0$ eV for $n = 2$, 3, ..., V − 1. A nearest neighbor hopping matrix element $V_{n,n\pm1} = 0.025$ eV was assumed. The reorganization energies are $\lambda_n = 0.1$ eV ($n = 1, 2, ..., N$), and $\lambda_D = \lambda_A = 0.05$ eV. Nuclear relaxation rate $\Lambda = 10^{12}$ s^{-1}, and the temperature is 300 K.

In Figure 2 we display the time-resolved fluorescence from the acceptor calculated using eqs 4.5 and 5.17−5.25 for varying numbers of sites N. The carrier frequency of the exciting pulse ω_0 is $\Omega_1 = 1.059$ eV. The ordinate coincides with the population of the acceptor because $\sum_k|\mu_{Ak}|^2$, $\sum_{k'}D_{k'}(\omega_0)$, and

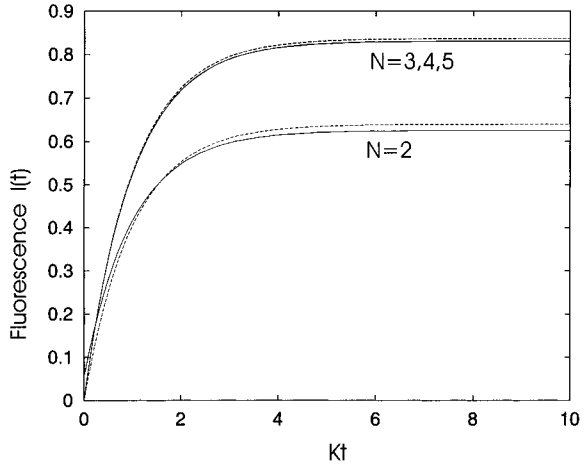

Figure 2. Time-resolved fluorescence $I(t)$ (which is proportional to the population of the acceptor) vs scaled time Kt for different values of the number of sites N, as indicated. Temperature is 300 K. Reorganization energies are $\lambda_n = 0.1$ eV ($n = 1, 2, ..., N$), $\lambda_D = 0.05$ eV, and $\lambda_A = 0.05$ eV. Nuclear relaxation rate Λ is 1 ps^{-1}. Electronic structure is as follows: $E_D = -1.25$ eV, $E_A = -2.29$ eV, $E_1 = -0.25$ eV, $E_N = -0.29$ eV, $E_n = 0.0$ eV, for $n = 2, 3, ..., N - 1$, and $V_{mn} = 0.025$ eV for $m = n - 1$ or $m = n + 1$; otherwise $V_{mn} = 0$. The carrier frequency of the exciting pulse ω_0 is $\Omega_1/\hbar$ ($\Omega_1 = 1.059$ eV). The population of the acceptor (eq 6.1) is plotted as well. Solid line: Time-resolved fluorescence $I(t)$. Dashed line: eq 6.1.

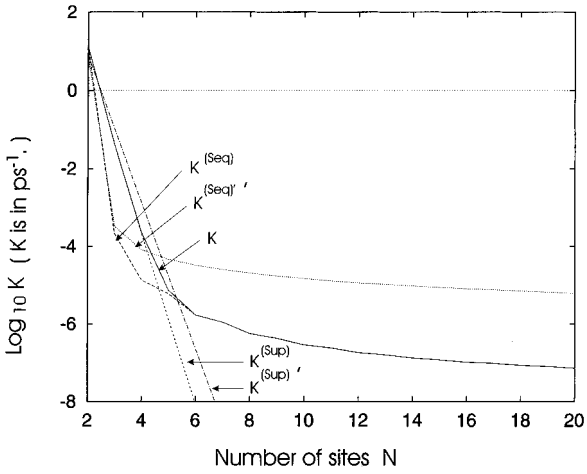

Figure 3. ET rate $\log_{10} K$ (K is in ps^{-1}.) vs number of sites N (the distance between the donor and the acceptor). Parameters are the same as Figure 2. Solid line: $\log_{10} K$. Dashed line: $\log_{10} K^{(seq)}$. Short dashed line: $\log_{10} K^{(sup)}$. Dotted line: $\log_{10} K^{(seq)}$. Dash−dotted line: $\log_{10} K^{(sup)'}$.

$\int_{-\infty}^{\infty}d\tau'\ |E(\tau')|^2/\hbar^2$ are normalized to 1. Since typical nuclear relaxation time scales (∼1 ps) are much shorter than the ET time scale ($\gtrsim$ 1 *ns*) in DNA, we neglect the short-time component which decays to zero on the nuclear relaxation time scale. The lowest eigenvalue of the matrix **K** (whose elements are $K_{qq'}$) is zero and gives the thermal equilibrium distribution. The second eigenvalue K dominates the relaxation to equilibrium at long times. In Figure 2 the scaled time Kt is used as an abscissa. Since for these parameters population of the bridge is negligible compared with the donor and acceptor, we expect the population of the acceptor $p_N(t)$ to be close to

$$p_N(t) = p_N(\infty)(1 - e^{-Kt}) \quad (6.1)$$

with

$$p_N(\infty) \equiv \frac{\exp\left(-\frac{\bar{\Omega}_{qN}}{k_B T}\right)}{\exp\left(-\frac{\bar{\Omega}_{q1}}{k_B T}\right) + \exp\left(-\frac{\bar{\Omega}_{qN}}{k_B T}\right)} \quad (6.2)$$

Here the delocalized state that goes to kth site state in the limit of $V_{mn} = 0$ is denoted by q_k.

Figure 2 shows that eq 6.1 indeed represents very well the fluorescence decay curves. K can thus be interpreted as a sum of the forward and backward ET rates. All time-resolved fluorescence curves are similar except for the $N = 2$ case (no bridge), where the two states, $|1\rangle$ and $|N\rangle$, are strongly mixed compared with the other cases. Hereafter we refer to K as the ET rate. The variation of this rate with the number of sites, N, using the parameters as in Figure 2 is shown in Figure 3. To analyze these results, we define the 2×2 superexchange $K^{(\mathrm{sup})}$ matrix.

$$\begin{pmatrix} K^{(\mathrm{sup})}_{q_1q_1} & K^{(\mathrm{sup})}_{q_1q_N} \\ K^{(\mathrm{sup})}_{q_Nq_1} & K^{(\mathrm{sup})}_{q_Nq_N} \end{pmatrix} \equiv \begin{pmatrix} -K_{q_Nq_1} & K_{q_1q_N} \\ K_{q_Nq_1} & -K_{q_1q_N} \end{pmatrix} \quad (6.3)$$

We further introduce the sequential rate matrix $\mathbf{K}^{(\mathrm{seq})}$.

$$K^{(\mathrm{seq})}_{qq'} \equiv 0 \quad \text{for } (q, q') = (q_1, q_N) \text{ or } (q, q') = (q_N, q_1) \quad (6.4)$$

$$K^{(\mathrm{seq})}_{qq'} \equiv K_{qq'} \quad \text{for } q \neq q', (q, q') \neq (q_1, q_N), \text{ and } (q, q') \neq (q_N, q_1) \quad (6.5)$$

$$K^{(\mathrm{seq})}_{qq'} \equiv \sum_{q'' (q'' \neq q)} K^{(\mathrm{seq})}_{q''q} \quad \text{for } q = q' \quad (6.6)$$

For $N = 2$ we define $K^{(\mathrm{sup})} \equiv K^{(\mathrm{seq})}$. We define the superexchange and sequential ET rates, $K^{(\mathrm{sup})}$ and $K^{(\mathrm{seq})}$, as the second lowest eigenvalues of $K^{(\mathrm{sup})}$ and $K^{(\mathrm{seq})}$, respectively. These quantities are plotted in Figure 3 as well. We see that for smaller N the superexchange transfer dominates, and for larger N the sequential transfer takes over.

To investigate the competition between the two mechanisms, we calculated the ET rate as a function of N, varying the energy gap between the donor site and the first bridge site, $\Delta E \equiv E_2 - E_1$. We kept all bridge energies to be the same, $E_n = 0.0$ eV for $n = 2, 3, ..., N - 1$, and the difference between the donor and the acceptor energies is the same as Figure 2, setting $E_1 = -\Delta E$ and $E_N = -\Delta E - 0.04$ eV. Figure 4 shows that as the energy gap ΔE is increased, the superexchange rate curve becomes steeper, and the sequential transfer rate slows down. The reorganization energy λ and temperature T are also varied (Figures 5 and 6). Figure 7 displays the variation of the rate with bridge size on a logarithmic scale. The rate varies as $N^{-\alpha}$ for large N, where the exponent α is not universal and depends on the parameters.

We next investigate the effect of energetic disorder of the bridge sites. E_n for $n = 3, ..., N - 1$ are modeled as independent random Gaussian variables whose average value is zero and variance $\delta = 2.5 \times 10^{-3}$ eV^2. This static disorder is sufficient to localize the exciton state within ~2 sites. Other parameters are identical to Figure 2.

At this point we would like to compare the present rates with those calculated perturbatively in the electronic coupling V_{nm}. The perturbative 2×2 superexchange rate matrix is $K^{(\mathrm{sup})'}$ with matrix elements

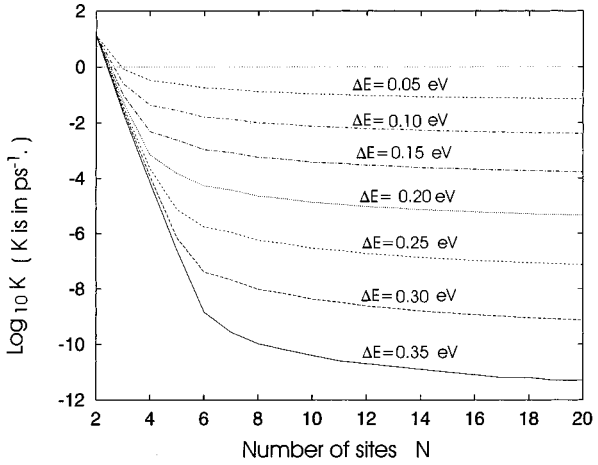

Figure 4. ET rate $\log_{10} K$ (K is in ps^{-1}.) vs number of sites N (the distance between the donor and the acceptor), for varying values of the energy gap ΔE, as indicated. Other parameters are the same as Figure 2.

$$K^{(\mathrm{sup})'}_{N1} \equiv |T_{N1}|^2 \sqrt{\frac{\pi}{\hbar^2 \bar{\lambda}_{N1} k_B T}} \exp\left[-\frac{(\bar{E}_N - \bar{E}_1 + \bar{\lambda}_{N1})^2}{4\bar{\lambda}_{N1} k_B T}\right] \quad (6.7)$$

$$K^{(\mathrm{sup})'}_{1N} \equiv |T_{N1}|^2 \sqrt{\frac{\pi}{\hbar^2 \bar{\lambda}_{1N} k_B T}} \exp\left[-\frac{(\bar{E}_N - \bar{E}_1 + \bar{\lambda}_{1N})^2}{4\bar{\lambda}_{1N} k_B T}\right] \quad (6.8)$$

$$K^{(\mathrm{sup})'}_{11} \equiv -K^{(\mathrm{sup})'}_{N1} \quad (6.9)$$

$$K^{(\mathrm{sup})'}_{N,N} \equiv -K^{(\mathrm{sup})'}_{1N} \quad (6.10)$$

where

$$\bar{E}_n \equiv E_n - \lambda_n \quad (6.11)$$

$$\bar{\lambda}_{nn'} \equiv \lambda_n + \lambda_{n'} \quad (6.12)$$

$$T_{N1} \equiv V_{NN-1} \cdots V_{43} \frac{1}{E - E_3} V_{32} \frac{1}{E - E_2} V_{21} \quad (6.13)$$

$$E \equiv \bar{E}_1 + \frac{(\bar{E}_N - \bar{E}_1 + \bar{\lambda}_{N1})^2}{4\bar{\lambda}_{N1}} \quad (6.14)$$

Similarly, the perturbative sequential rate matrix $K^{(\mathrm{seq})'}$ is given by

$$K^{(\mathrm{seq})'}_{nn'} \equiv |V_{nn'}|^2 \sqrt{\frac{\pi}{\hbar^2 \bar{\lambda}_{nn'} k_B T}} \exp\left[-\frac{(\bar{E}_N - \bar{E}_1 + \bar{\lambda}_{nn'})^2}{4\bar{\lambda}_{nn'} k_B T}\right] \quad \text{for} \quad n \neq n' \quad (6.15)$$

$$K^{(\mathrm{seq})'}_{nn'} \equiv \sum_{n'' (n'' \neq n)} K^{(\mathrm{seq})'}_{n''n} \quad \text{for} \quad n = n' \quad (6.16)$$

For $N = 2$ we define $K^{(\mathrm{sup})'} \equiv K^{(\mathrm{seq})'}$. This perturbation theory has been used to investigate the competition between the superexchange and sequential transfer.[20−23] The superexchange ET rate $K^{(\mathrm{sup})'}$ and the sequential ET rate $K^{(\mathrm{seq})'}$ defined as the second lowest eigenvalues of $\mathbf{K}^{(\mathrm{sup})'}$ and $\mathbf{K}^{(\mathrm{seq})'}$, respectively, are shown in Figure 8 as well. We note that $K^{(\mathrm{sup})'}$ is very close to $K^{(\mathrm{sup})}$ and $K^{(\mathrm{seq})'}$ is very close to $K^{(\mathrm{seq})}$. This is not the case when the bridge eigenstates are delocalized, as illustrated in Figure 3.

Finally, the calculated time- and frequency-resolved fluorescence is displayed in Figure 9. All parameters are the same as in Figure 2 except for the number of sites, N, which is 10.

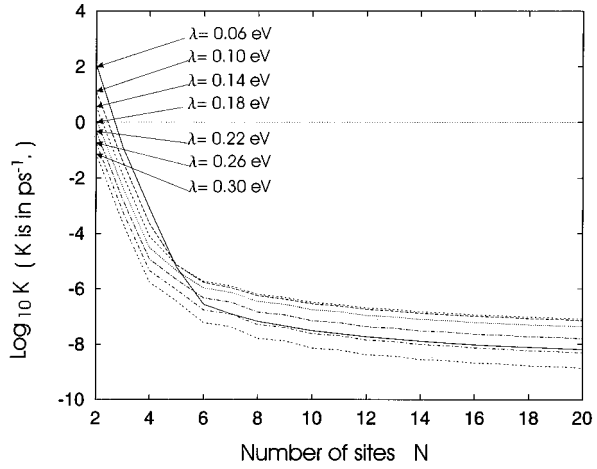

Figure 5. Same as Figure 4, except that the reorganization energy λ is varied, as indicated where $\lambda_n = \lambda$ ($n = 1, 2, ..., N$), $\lambda_D = \lambda/2$, and $\lambda_A = \lambda/2$.

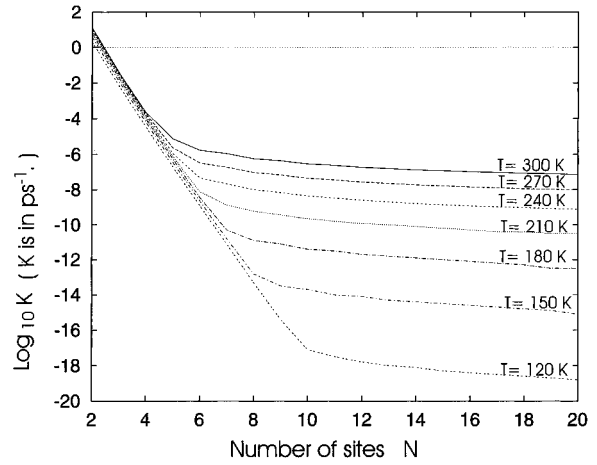

Figure 6. Same as Figure 4, except that the temperature T is varied, as indicated.

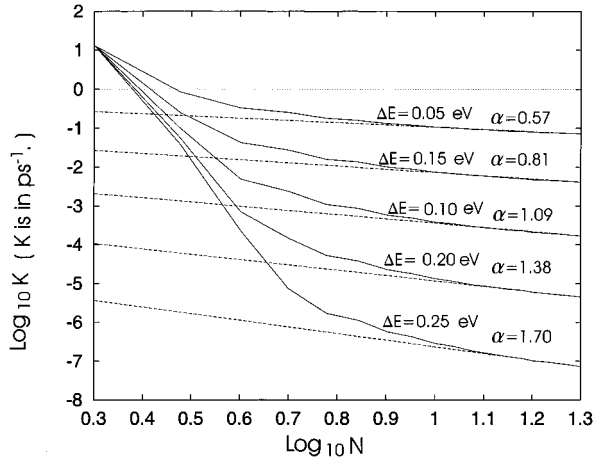

Figure 7. Same as Figure 4, but abscissa in logarithmic scale N. Solid line: $\log_{10} K$. Dashed line: $-\alpha \log_{10} N$. The exponents α are listed in this figure.

Assuming that Nth electronic state is well-localized on the acceptor, time- and frequency-resolved fluorescence $S(t, \omega_s)$ can be approximated as,

$$S(t, \omega_s) = I(t)\, W(\omega_s) \tag{6.17}$$

where $W(\omega_s)$ is fluorescence from an isolated acceptor,

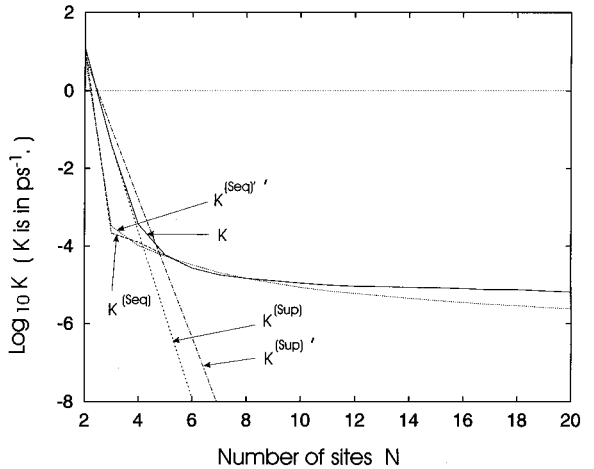

Figure 8. Same as Figure 2, but disorder is included in the bridge site energies. Each E_n for $n = 2, 3, ..., N - 1$ has Gaussian distribution with average 0.0 and variance 0.05 eV.

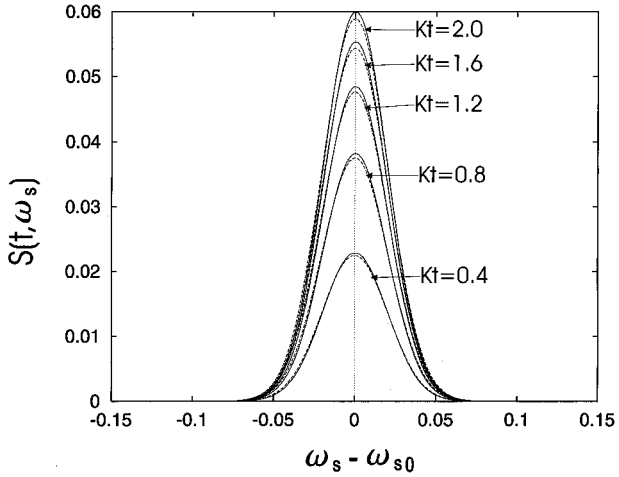

Figure 9. Time- and frequency-resolved fluorescence $S(t, \omega_s)$. The parameters are the same as in Figure 2, but the number of sites N is 10. The abscissa is $\hbar(\omega_s - \omega_{AN})$, where ω_{AN} is the frequency of maximum fluorescence from an isolated acceptor, and the unit of the ordinate is arbitrary. Time t is varied from 0 to 2 K^{-1} where $K = 0.29$ [μs^{-1}], as indicated. Solid line: eq 4.4. Dashed line: the approximation (eq 6.17).

$$W(\omega_s) = \left(\frac{\pi\hbar^2}{\lambda_{AN} k_B T}\right)^{1/2} \exp\left[-\frac{(\hbar\omega_{AN} - \hbar\omega_s)^2}{4\bar{\lambda}_{AN} k_B T}\right] \tag{6.18}$$

with $\lambda_{AN} \equiv \lambda_A + \lambda_N - 2\sqrt{\lambda_A \lambda_N}$ and $\hbar\omega_{AN} \equiv (\Omega_A - \lambda_A) - (\Omega_N - \lambda_N) + \bar{\lambda}_{AN}$. In general, the fluorescence line shape varies with time and may not be factorized in the form of eq 6.17.

VII. Discussion

In the present theory the ET system is modeled by a Hamiltonian describing localized electronic states in the site representation, coupled to each other and to harmonic nuclear degrees freedom. To include higher order contributions in the electronic couplings among sites, the eigenstates of the electronic part of Hamiltonian are used as a basis set. In this representation the nuclei couple to diagonal as well as off-diagonal elements of the electronic Hamiltonian. Only the latter couplings are treated perturbatively. This treatment of nuclear modes incorporates the reorganization energy as well as memory effects of nuclear modes. The photoexcitation of the donor and the resulting fluorescence are formulated microscopically, without

invoking the common assumption that the excited donor state is equilibrated initially. Using the present theory, the effects of the bridge size, the energy gap between the donor/acceptor and the bridge, the reorganization energies, and the temperature on the competition between the superexchange and sequential transfer were investigated, and the time- and frequency-resolved fluorescence was calculated.

Effects of solvation on long-range ET in DNA have been studied recently in ref 19 using the density matrix approach.[20] A single high-frequency vibrational oscillator was coupled to the electronic states of the donor/bridge/acceptor systems. The oscillator and the electronic states were then coupled to other nuclear bath modes. Eliminating these external degrees of freedom and applying the Redfield equation of motion, the time evolution of ET in DNA including nuclear dynamics was calculated. The Redfield equation retains terms only up to second order in the system−bath coupling, and the bath time scale is assumed to be much shorter than the ET process. Consequently, the reorganization energy (which originates from slow nuclear modes) and the finite time scale of the nuclear modes except for the high-frequency mode were not included.

Finally we comment on the relation between the present calculations which use the delocalized electronic basis set and the direct perturbative calculation of the rate in intermolecular electronic coupling. We expect the two to be similar if the coupling is weak, $|\Omega'_n - \Omega'_{n'}| \gg V_{nn'}$. Expanding the transfer rate between the qth and q'th excitons in $V_{nn'}$, we obtain

$$K_{qq'} = \left(1 + \frac{\lambda_{n'} - \lambda_n}{E_{n'} - E_n}\right)^2 K_{nn'} \tag{7.1}$$

where

$$K_{nn'} \equiv \left(\frac{V_{nn'}}{\hbar}\right)^2 \left(\frac{\pi\hbar^2}{(\lambda_n + \lambda_{n'})k_B T}\right)^{1/2} \times \left[-\frac{\{(E_n - \lambda_n) - (E_{n'} - \lambda_{n'}) + \lambda_n + \lambda_{n'}\}^2}{4(\lambda_n + \lambda_{n'})k_B T}\right] \tag{7.2}$$

is the Marcus rate between the nth and n'th states. The qth and q'th states go to the nth and n'th states, respectively, in the $V_{nn'} = 0$ limit. Here

$$\lambda_{qq,qq} = \lambda_n \tag{7.3}$$

$$\lambda_{q'q',q'q'} = \lambda_{n'} \tag{7.4}$$

$$\lambda_{q'q',q'q'} = \left(\frac{V_{nn'}}{E_n - E_{n'}}\right)^2 (\lambda_n + \lambda_{n'}) \tag{7.5}$$

$$\lambda_{q'q,qq} = \frac{V_{nn'}}{E_n - E_{n'}}\lambda_n \tag{7.6}$$

$$\lambda_{qq',q'q'} = \frac{V_{nn'}}{E_{n'} - E_n}\lambda_{n'} \tag{7.7}$$

$$\bar{\lambda}_{qq'} = \lambda_n + \lambda_{n'} \tag{7.8}$$

When V_{mn} is weak, the two perturbation theories give similar expressions for the rate except for different prefactors. The two expressions coincide when $|E_{n'} - E_n| \gg |\lambda_{n'} - \lambda_n|$.

Acknowledgment. We gratefully acknowledge the support of the National Science Foundation, the U.S. Air Force Office of Scientific Research, and the NSF Center for Photoinduced Charge Transfer.

Appendix A: Quantities Appearing in Eq 3.8

The auxiliary functions appearing in eq 3.8 are given by

$$D_k^{\mathrm{L}}(\tau) = \mu_{Dk}{}^2 \exp\left[-\frac{\mathrm{i}}{\hbar}\Omega_k\tau - g_{kk,kk}(\tau)\right] \tag{A1}$$

$$W_k^{\mathrm{L}}(\tau) = \mu_{Ak}{}^2 \exp\left[-\frac{\mathrm{i}}{\hbar}(\Omega_A - \Omega_k)\tau + 2\frac{\mathrm{i}}{\hbar}(\lambda_{kk,Y} - \lambda_{kk,kk})\tau - g_{kk,kk}(\tau) - g_{Y,Y}(\tau) + 2g_{kk,Y}(\tau)\right] \tag{A2}$$

$$\tilde{S}^{(\mathrm{st})}(t,\tau) = \int_{-\infty}^{t}\mathrm{d}\tau' \int_{-\infty}^{t+\tau}\mathrm{d}\tau'' F_2(\tau'', t+\tau, t, \tau')\frac{\epsilon(\tau')}{\hbar}\frac{\epsilon(\tau'')}{\hbar} - \theta(\tau)\sum_k \int_{-\infty}^{t}\mathrm{d}\tau' \int_{-\infty}^{\tau'}\mathrm{d}\tau'' W_k^{\mathrm{L}}(\tau) D_k(\tau' - \tau'')\frac{\epsilon(\tau')}{\hbar}\frac{\epsilon(\tau'')}{\hbar} - \theta(-\tau)\sum_k \int_{-\infty}^{t+\tau}\mathrm{d}\tau' \int_{-\infty}^{\tau'}\mathrm{d}\tau'' W_k^{\mathrm{L}}(\tau) D_k(\tau' - \tau'')\frac{\epsilon(\tau')}{\hbar}\frac{\epsilon(\tau'')}{\hbar} \tag{A3}$$

where the correlation function F_2 defined by eq 3.7 is calculated under the assumption that $H_1 = 0$ and has the form[30]

$$F_2(\tau_4, \tau_3, \tau_2, \tau_1) \equiv \sum_{kk'} \mu_{Dk}\mu_{Dk'}\mu_{Ak}\mu_{Ak'} \exp[-f^{(2)}_{kk',Y}(\tau_4, \tau_3, \tau_2, \tau_1)] \times \exp\left[-\frac{\mathrm{i}}{\hbar}\Omega_k(\tau_2 - \tau_1) - \frac{\mathrm{i}}{\hbar}\Omega_A(\tau_3 - \tau_2) - \frac{\mathrm{i}}{\hbar}\Omega_{k'}(\tau_4 - \tau_3)\right] \tag{A4}$$

and

$$\lambda_{\mu,\nu} \equiv -\hbar \lim_{\tau\to\infty} \mathrm{Im}\left[\frac{dg_{\mu,\nu}(\tau)}{\mathrm{d}\tau}\right] \tag{A5}$$

The function $f^{(2)}$ in eq A4 is given by

$$f^{(2)}_{kk',Y}(\tau_4, \tau_3, \tau_2, \tau_1) = g_{kk,kk}(\tau_2 - \tau_1) - g_{kk,Y}(\tau_2 - \tau_1) + g_{kk,Y}(\tau_3 - \tau_1) - g_{kk,k'k'}(\tau_3 - \tau_1) + g_{kk,k'k'}(\tau_4 - \tau_1) - g_{kk,Y}(\tau_3 - \tau_2) + g_{kk,k'k'}(\tau_3 - \tau_2) - g_{kk,k'k'}(\tau_4 - \tau_2) + g_{Y,Y}(\tau_3 - \tau_2) - g_{k'k',Y}(\tau_3 - \tau_2) + g_{k'k',Y}(\tau_4 - \tau_2) - g_{k'k',Y}(\tau_4 - \tau_3) + g_{k'k',k'k'}(\tau_4 - \tau_3) \tag{A6}$$

Appendix B: ET Rates for a Finite Solvent Time Scale

In this Appendix we present expressions for doorway/window functions and the kernel $K_{qq'}$ for the overdamped Brownian oscillator model for the spectral density, which do not assume the static limit. A confluent hypergeometric function is used to derive the expressions.

For $\tau \geq 0$ we have

$$D_k^{\mathrm{L}}(\tau) = {\mu_{Dk}}^2 \exp\left[-\mathrm{i}\bar{\omega}_{Dk}\tau - \frac{\bar{\lambda}_{Dk}}{\lambda} g(\tau)\right] \quad \text{(B1)}$$

$$W_k^{\mathrm{L}}(\tau) = {\mu_{Ak}}^2 \exp\left[-\mathrm{i}\bar{\omega}_{Ak}\tau - \frac{\bar{\lambda}_{Ak}}{\lambda} g(\tau)\right] \quad \text{(B2)}$$

$$K_{qq'}^{\mathrm{L}}(\tau) = (A_{qq'}\mathrm{e}^{-2\Lambda\tau} + B_{qq'}\mathrm{e}^{-\Lambda\tau} + C_{qq'}) \times \exp\left[-\mathrm{i}\bar{\omega}_{qq'\tau} - \frac{\bar{\lambda}_{qq'}}{\lambda} g(\tau)\right] \quad \text{(B3)}$$

where

$$\bar{\omega}_{Dk} \equiv \frac{\Omega_k}{\hbar} \quad \text{(B4)}$$

$$\bar{\lambda}_{Dk} \equiv \lambda_{kk,kk} \quad \text{(B5)}$$

$$\bar{\omega}_{Ak} \equiv \frac{1}{\hbar}(\Omega_A - \Omega_k) - \frac{2}{\hbar}(\lambda_{kk,Y} - \lambda_{kk,kk}) \quad \text{(B6)}$$

$$\bar{\lambda}_{Ak} \equiv \lambda_{kk,kk} + \lambda_{Y,Y} - 2\lambda_{kk,Y} \quad \text{(B7)}$$

$$\bar{\omega}_{qq'} \equiv \frac{1}{\hbar}(\Omega_q - \Omega_{q'}) + \frac{2}{\hbar}(\lambda_{q'q',q'q'} - \lambda_{qq,q'q'}) \quad \text{(B8)}$$

$$\bar{\lambda}_{qq'} \equiv \lambda_{qq,qq} + \lambda_{q'q',q'q'} - \lambda_{q'q',qq} - \lambda_{qq,q'q'} \quad \text{(B9)}$$

$$A_{qq'} \equiv -\frac{z^2}{\lambda^2}\Lambda^2(\lambda_{q'q,q'q'} - \lambda_{q'q,qq})(\lambda_{q'q',qq'} - \lambda_{qq,qq'}) \quad \text{(B10)}$$

$$B_{qq'} \equiv \frac{z}{\lambda}\Lambda^2\lambda_{qq',q'q} + \frac{z}{\lambda}\Lambda(\lambda_{q'q,q'q'} - \lambda_{q'q,qq}) \times \left[\frac{z}{\lambda}\Lambda(\lambda_{q'q',qq'} - \lambda_{qq,qq'}) + 2\frac{\mathrm{i}}{\hbar}\lambda_{qq',q'q'}\right] + \frac{z}{\lambda}\Lambda(\lambda_{q'q',qq'} - \lambda_{qq,qq'}) \times \left[\frac{z}{\lambda}\Lambda(\lambda_{q'q,q'q'} - \lambda_{q'q,qq}) + 2\frac{\mathrm{i}}{\hbar}\lambda_{q'q,q'q'}\right] \quad \text{(B11)}$$

$$C_{qq'} \equiv -\left[\frac{z}{\lambda}\Lambda(\lambda_{q'q,q'q'} - \lambda_{q'q,qq}) + 2\frac{\mathrm{i}}{\hbar}\lambda_{q'q,q'q'}\right] \times \left[\frac{z}{\lambda}\Lambda(\lambda_{q'q',qq'} - \lambda_{qq,qq'}) + 2\frac{\mathrm{i}}{\hbar}\lambda_{qq',q'q'}\right] \quad \text{(B12)}$$

Using eqs B1−B12, we obtain[27,31]

$$D_k(\omega) = \frac{2\mathrm{Re}\,{\mu_{Dk}}^2}{\Lambda\dfrac{\bar{\lambda}_{Dk}}{\lambda}z - \mathrm{i}(\omega - \bar{\omega}_{Dk})} \sum_{m=0}^{\infty} \frac{\left(\dfrac{\bar{\lambda}_{Dk}}{\lambda}z\right)^m}{\left(\dfrac{\bar{\lambda}_{Dk}}{\lambda}z - \mathrm{i}(\omega - \bar{\omega}_{Dk})/\Lambda + 1\right)_m} \quad \text{(B13)}$$

$$W_k(\omega) = \frac{2\mathrm{Re}\,{\mu_{Ak}}^2}{\Lambda\dfrac{\bar{\lambda}_{Ak}}{\lambda}z - \mathrm{i}(\omega - \bar{\omega}_{Ak})} \sum_{m=0}^{\infty} \frac{\left(\dfrac{\bar{\lambda}_{Ak}}{\lambda}z\right)^m}{\left(\dfrac{\bar{\lambda}_{Ak}}{\lambda}z - \mathrm{i}(\omega - \bar{\omega}_{Ak})/\Lambda + 1\right)_m} \quad \text{(B14)}$$

$$K_{qq'} = 2\mathrm{Re}\left[A_{qq'}\frac{1}{\Lambda\dfrac{\bar{\lambda}_{qq'}}{\lambda}z + 2\Lambda + \mathrm{i}\bar{\omega}_{qq'}} \sum_{m=0}^{\infty} \frac{\left(\dfrac{\bar{\lambda}_{qq'}}{\lambda}z\right)^m}{\left(\dfrac{\bar{\lambda}_{qq'}}{\lambda}z + \mathrm{i}\bar{\omega}_{qq'}/\Lambda + 3\right)_m} + B_{qq'}\frac{1}{\Lambda\dfrac{\bar{\lambda}_{qq'}}{\lambda}z + \Lambda + \mathrm{i}\bar{\omega}_{qq'}} \sum_{m=0}^{\infty} \frac{\left(\dfrac{\bar{\lambda}_{qq'}}{\lambda}z\right)^m}{\left(\dfrac{\bar{\lambda}_{qq'}}{\lambda}z + \mathrm{i}\bar{\omega}_{qq'}/\Lambda + 2\right)_m} + C_{qq'}\frac{1}{\Lambda\dfrac{\bar{\lambda}_{qq'}}{\lambda}z + \mathrm{i}\bar{\omega}_{qq'}} \sum_{m=0}^{\infty} \frac{\left(\dfrac{\bar{\lambda}_{qq'}}{\lambda}z\right)^m}{\left(\dfrac{\bar{\lambda}_{qq'}}{\lambda}z + \mathrm{i}\bar{\omega}_{qq'}/\Lambda + 1\right)_m}\right] \quad \text{for} \quad q \neq q' \quad \text{(B15)}$$

$$K_{qq'} = -\sum_{q''}^{q''\neq q'} K_{q''q'} \quad \text{for} \quad q = q' \quad \text{(B16)}$$

Here $(a)_m$ is defined as

$$(a)_0 \equiv 1 \quad \text{(B17)}$$

$$(a)_m \equiv a(a+1)\ldots(a+m-1) \quad \text{(B18)}$$

Appendix C: Alternative Expressions for ET Rates

In this section alternative expressions for ET rates which are not limited to the static limit are derived using a Taylor expansion for an exponential function in another exponential function that appears in the expressions of DW functions and the kernel $K_{qq'}$ (eqs B1−B3).

For $\tau \geq 0$ we have

$$D_k^{\mathrm{L}}(\tau) = {\mu_{Dk}}^2 \exp[a_{Dk}\tau + b_{Dk}\mathrm{e}^{-\Lambda\tau} - b_{Dk}] \quad \text{(C1)}$$

$$= {\mu_{Dk}}^2 \mathrm{e}^{-b_{Dk}} \sum_{n=0}^{\infty} \frac{b_{Dk}^n}{n!} \exp[(a_{Dk} - n\Lambda)\tau] \quad \text{(C2)}$$

$$W_k^{\mathrm{L}}(\tau) = {\mu_{Ak}}^2 \exp[a_{Ak}\tau + b_{Ak}\mathrm{e}^{-\Lambda\tau} - b_{Ak}] \quad \text{(C3)}$$

$$= {\mu_{Ak}}^2 \mathrm{e}^{-b_{Ak}} \sum_{n=0}^{\infty} \frac{b_{Ak}^n}{n!} \exp[(a_{Ak} - n\Lambda)\tau] \quad \text{(C4)}$$

$$K_{qq'}^{\mathrm{L}}(\tau) = \exp[a_{qq'}\tau + b_{qq'}\mathrm{e}^{-\Lambda\tau} - b_{qq'}](A_{qq'}\mathrm{e}^{-2\Lambda\tau} + B_{qq'}\mathrm{e}^{-\Lambda\tau} + C_{qq'}) \quad \text{(C5)}$$

$$= \mathrm{e}^{-b_{qq'}} \sum_{n=0}^{\infty} \frac{b_{qq'}^n}{n!} \exp[(a_{qq'} - n\Lambda)\tau](A_{qq'}\mathrm{e}^{-2\Lambda\tau} + B_{qq'}\mathrm{e}^{-\Lambda\tau} + C_{qq'}) \quad \text{(C6)}$$

where

$$a_{Dk} \equiv -\frac{\mathrm{i}}{\hbar}\Omega_k - \lambda_{kk,kk}\frac{z}{\lambda}\Lambda \tag{C7}$$

$$b_{Dk} \equiv -\lambda_{kk,kk}\frac{z}{\lambda} \tag{C8}$$

$$a_{Ak} \equiv -\frac{\mathrm{i}}{\hbar}(\Omega_A - \Omega_k) + 2\frac{\mathrm{i}}{\hbar}(\lambda_{kk,Y} - \lambda_{kk,kk}) + (-\lambda_{kk,kk} - \lambda_{Y,Y} + 2\lambda_{kk,Y})\frac{z}{\lambda}\Lambda \tag{C9}$$

$$b_{Ak} \equiv (-\lambda_{kk,kk} - \lambda_{Y,Y} + 2\lambda_{kk,Y})\frac{z}{\lambda} \tag{C10}$$

$$a_{qq'} \equiv -\frac{\mathrm{i}}{\hbar}(\Omega_q - \Omega_{q'}) - 2\frac{\mathrm{i}}{\hbar}(\lambda_{q'q',q'q'} - \lambda_{qq,q'q'}) - (\lambda_{qq,qq} + \lambda_{q'q',q'q'} - \lambda_{q'q',qq} - \lambda_{qq,q'q'})\frac{z}{\lambda}\Lambda \tag{C11}$$

$$b_{qq'} \equiv -(\lambda_{qq,qq} + \lambda_{q'q',q'q'} - \lambda_{q'q',qq} - \lambda_{qq,q'q'})\frac{z}{\lambda} \tag{C12}$$

Using eqs B10−B12 and C1−C12, we obtain

$$D_k(\omega) = -2\mathrm{Re}\,\mu_{Dk}{}^2 \mathrm{e}^{-b_{Dk}} \sum_{n=0}^{\infty} \frac{b_{Dk}^n}{n!} \frac{1}{a_{Dk} - n\Lambda + \mathrm{i}\omega} \tag{C13}$$

$$W_k(\omega) = -2\mathrm{Re}\,\mu_{Ak}{}^2 \mathrm{e}^{-b_{Ak}} \sum_{n=0}^{\infty} \frac{b_{Dk}^n}{n!} \frac{1}{a_{Dk} - n\Lambda + \mathrm{i}\omega} \tag{C14}$$

$$K_{qq'} \equiv -2\mathrm{Re}\,\mathrm{e}^{-b_{qq'}} \sum_{n=0}^{\infty} \frac{b_{qq'}^n}{n!} \left(A_{qq'} \frac{1}{a_{qq'} - (n+2)\Lambda} + B_{qq'} \frac{1}{a_{qq'} - (n+1)\Lambda} + C_{qq'} \frac{1}{a_{qq'} - n\Lambda} \right) \quad \text{for} \quad q \neq q' \tag{C15}$$

References and Notes

(1) Bolton, J. R.; Mataga, N.; McLendon, G. *Electron Transfer in Inorganic, Organic and Biological System*; ACS Advances in Chemistry Series No. 228; Bolton, J. R., Mataga, N., McLendon, G., Eds.; American Chemical Society: Washington, DC, 1991.

(2) Sigel, H.; Sigel, A. *Electron Transfer Reactions in Metalloproteins*; Sigel, H., Sigel, A., Eds.; Marcel Dekker: New York, 1991.

(3) Breton, J.; Vermeglio, A. *The Photosynthetic Bacterial Reaction Center*: *Structure and Dynamics*; Breton, J., Vermeglio, A., Eds.; Plenum Press, New York, 1988.

(4) Palmer, G. *Long-Range Electron Transfer in Biology*; Palmer, G., Ed.; Springer-Verlag: Berlin, 1991.

(5) Marcus, R. A.; Sutin, N. *Biochim. Biophys. Acta* **1985**, *811*, 265.

(6) Speiser, S. *Chem. Rev.* **1996**, *96*, 1953.

(7) Murphy, C. J.; Arkin, M. R.; Jenkins, Y.; Ghatlia, N. D.; Bossmann, S. H.; Turro, N. J.; Barton, J. K. *Science* **1993**, *262*, 1025.

(8) Arkin, M. R.; Stemp, E. D. A.; Holmlin, R. E.; Barton, J. K.; Hormann, A.; Olson, E. J. C.; Barbara, P. F. *Science* **1996**, *273*, 475.

(9) Brun, A. M.; Harriman, A. *J. Am. Chem. Soc.* **1992**, *114*, 3656.

(10) Brun, A. M.; Harriman, A. *J. Am. Chem. Soc.* **1994**, *116*, 10383.

(11) Lincoln, P.; Tuite, E.; Norden, B. *J. Am. Chem. Soc.* **1997**, *119*, 1454.

(12) Olson, E. J. C.; Hu, D.; Hormann, A.; Barbara, P. F. *J. Phys. Chem. B* **1997**, *101*, 299.

(13) Meade, T. J.; Kayyem, J. F. *Angew. Chem., Int. Ed. Engl.* **1995**, *34*, 352.

(14) Park, H. W.; Kim, S. T.; Sancar, A.; Deisenhofer, J. *Science* **1995**, *268*, 1866.

(15) Clery, D. *Science* **1995**, *267*, 1270.

(16) McConnell, H. M. *J. Chem. Phys.* **1961**, *35*, 508.

(17) Bassler, H. *Disorder Effects on Relaxation Process*; Richert, R., Blumen, A., Eds.; Springer: Berlin, 1994.

(18) Priyadarshy, S.; Risser, S. M.; Beratan, D. N. *J. Phys. Chem.* **1996**, *100*, 17678.

(19) Felts, A. K.; Pollard, W. T.; Friesner, R. A. *J. Phys. Chem.* **1995**, *99*, 2929.

(20) Hu, Y.; Mukamel, S. *Chem. Phys. Lett.* **1989**, *160*, 410; *J. Chem. Phys.* **1989**, *91*, 6973.

(21) Sumi, H.; Kakitani, T. *Chem. Phys. Lett.* **1996**, *252*, 85.

(22) Egger, R.; Mak, C. H. *J. Chem. Phys.* **1994**, *98*, 9903. Egger, R.; Mak, C. H.; Weiss, *U. Phys. Rev. E* **1994**, *50*, R655.

(23) Kühn, O.; Rupasov, V.; Mukamel, S. *J. Chem. Phys.* **1996**, *104*, 5821.

(24) Skourtis, S. S.; Mukamel, S. *Chem. Phys.* **1995**, *197*, 367.

(25) Marcus, R. A. *Chem. Phys. Lett.* **1987**, *133*, 471; *Chem. Phys. Lett.* **1988**, *146*, 13.

(26) Bixon, M.; Jortner, J.; Michel-Beyerle, M. E. *Chem. Phys.* **1995**, *197*, 389.

(27) Mukamel, S. *Principles of Nonlinear Optical Spectroscopy*; Oxford: New York, 1995.

(28) Mukamel, S. *Phys. Rev. A* **1983**, *28*, 3480.

(29) Zwanzig, R. *Statistical Mechanics of Irreversibility*, Vol. 3 of Lectures in Theoretical Physics; Interscience: New York, 1961.

(30) Meier, T.; Chernyak, V.; Mukamel, S. *J. Chem. Phys.* **1997**, *107*, 8759. Zhang, W. M.; Meier, T.; Chernyak, V.; Mukamel, S. *Philos. Trans. R. Soc. London, Ser. A*, in press.

(31) Abramowitz, A.; Stegum, A. R. *Handbook of Mathematical Function*; Dover: New York, 1970.